RNA PROCESSING AND MODIFICATIONS

OPINION

RNA modifications and structures cooperate to guide RNA–protein interactions

Cole J.T. Lewis, Tao Pan and Auinash Kalsotra

Abstract | An emerging body of evidence indicates that post-transcriptional gene regulation relies not only on the sequence of mRNAs but also on their folding into intricate secondary structures and on the chemical modifications of the RNA bases. These features, which are highly dynamic and interdependent, exert direct control over the transcriptome and thereby influence many aspects of cell function. Here, we consider how the coupling of RNA modifications and structures shapes RNA–protein interactions at different steps of the gene expression process.

Gene expression relies on the intricate coordination of precursor mRNA (pre-mRNA) processing stages, which include capping, splicing and polyadenylation, as well as the export of mature transcripts to the cytoplasm for translation. How do cells exert tight spatiotemporal control over these multistep processes? Coupling of nuclear and cytosolic processes can be accomplished through two distinct mechanisms. First, RNA-binding proteins (RBPs) that shuttle between the nucleus and the cytoplasm can bind their target transcripts in the nucleus to influence their processing. An excellent example of this is the serine/arginine-rich (SR) proteins, which are RBPs that were initially found to have diverse roles in splicing and were later found to be important for transcription elongation, polyadenylation, mRNA export and translation[1–5]. Second, nuclear processing, which includes splicing and polyadenylation as well as dynamic changes in RNA chemical modifications and secondary structures (discussed below), can facilitate downstream associations with RBPs in the cytoplasm and thereby affect mRNA translation and decay.

As RBPs link multiple steps of gene expression, factors governing their binding to target RNAs must be considered in order to understand how coupling between the different processing steps is achieved. The mRNA sequence is often insufficient to drive protein binding, as RBP consensus motifs are highly overrepresented compared with the incidence of actual binding[6–8], which indicates that additional features are responsible for determining the specificity of protein–RNA interactions in cells. Recent studies have revealed that post-transcriptional modifications of mRNA through the addition or removal of chemical groups (together comprising the epitranscriptome) can expand the information encoded by RNA[9]. As we discuss below, RNA modifications, which are dynamic and reversible, can modulate protein–RNA interactions and mediate rapid responses to environmental changes. In addition to the panoply of chemical modifications, mRNAs also fold into intricate secondary structures. Until recently, the structural aspect of the transcriptome was largely unexplored owing to technical limitations. The development of new transcriptome-wide approaches to study RNA structure *in vivo* has unravelled the plasticity, complexity and functionality of mRNA structures[10–12].

In this Opinion article, we discuss recent findings that demonstrate the functional coupling and interdependence of mRNA modifications and structures (the editing of adenosine to inosine[13] and cytidine to uridine[14] are not discussed here), and we provide an updated view of gene expression that incorporates the dynamics and physiological relevance of these RNA features and how they shape binding by RBPs.

RNA modifications

The epitranscriptome is shaped through the activity of evolutionarily conserved factors that encode (writers), decode (readers) and remove (erasers) various chemical modifications of RNA bases (FIG. 1). More than 100 distinct types of RNA modifications have been found to date[15], and more will likely be identified. Although most modifications — which include N^6-methyladenosine (m^6A), 5-methylcytosine (m^5C), N^1-methyladenosine (m^1A) and pseudouridine (Ψ) — were originally identified in the highly abundant ribosomal RNAs (rRNAs), transfer RNAs (tRNAs) and small nuclear RNA (snRNAs)[16,17], recent advances in sequencing and mass spectrometry enabled their detection and characterization in the relatively lowly expressed mRNAs. Genome-wide analyses, coupled with gain- and loss-of-function studies of readers, writers and erasers, have expanded the number of mRNA modifications in eukaryotic transcriptomes, annotated their abundance and distribution along transcripts, mapped the modification sites that are conserved between species, unravelled changes in modification abundance and position in response to environmental changes, demonstrated their impact on mRNA processing, stability and translation, and revealed the physiological consequences of modification dynamics.

RNA modifications expand the splicing code. The 'splicing code' represents the full set of RNA features that directly influence pre-mRNA splicing[18]. Although sequence elements such as the binding motifs of RBPs have been studied extensively, evidence now indicates that RNA modifications also have a role in determining the splicing code. Of the internal mRNA modifications (that is, excluding the 5′ 7-methylguanosine cap and 3′ poly(A) tail), m^6A is the most prevalent, accounting for approximately 80% of all

a

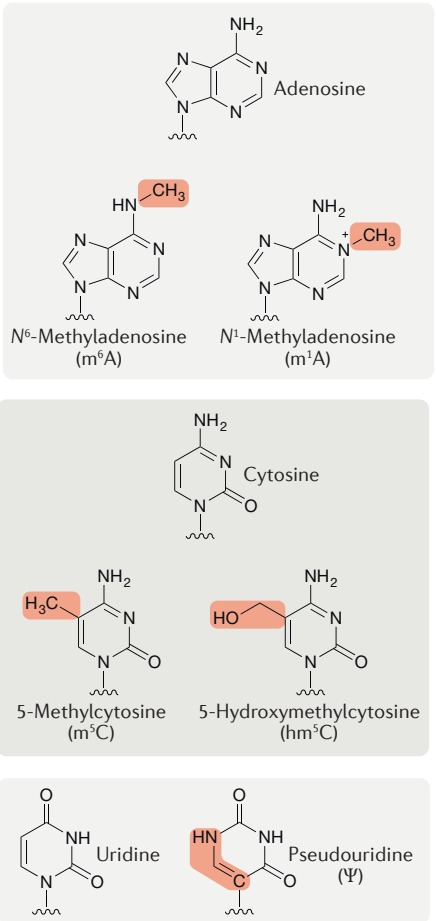

b

Modification	Writer	Eraser	Reader
N^6-Methyladenosine	• Methyltransferase-like 3 (METTL3) and METTL14 • Wilms tumour 1-associated protein (WTAP) • RNA-binding motif protein 15 (RBM15) and RBM15B • Protein virilizer homologue (KIAA1429)	• AlkB homologue 5 (ALKBH5) • Fat mass and obesity-associated protein (FTO)	• YTH domain family proteins 1–3 (YTHDF1–3) • YTH domain-containing protein 1 (YTHDC1) • Eukaryotic translation initiation factor 3 (eIF3) complex • Heterogeneous nuclear ribonucleoproteins A2/B1 (HNRNPA2B1) and HNRNPC • Serine/arginine-rich splicing factor 2 (SRSF2)
N^1-Methyladenosine	Unknown	ALKBH3	Unknown
5-Methylcytosine	• NOL1/NOP2/Sun domain family member 2 (NSUN2) • DNA methyltransferase-like protein 2 (DNMT2)	Unknown	Unknown
5-Hydroxymethylcytosine*	• Ten-eleven translocation protein 1–3 (TET1–TET3)	Unknown	Unknown
Pseudouridine	• Pseudouridine synthase 1–4 (PUS1–PUS4), PUS6, PUS7, PUS9 • Dyskeratosis congenita protein 1 (DKC1)	Unknown	Unknown

*5-Hydroxymethylcytosine is formed by the hydroxylation of 5-methylcytosine.

Figure 1 | **RNA modifications and their writers, erasers and readers. a** | Chemical structures of unmodified and modified RNA bases. **b** | The writers, readers and erasers of RNA modifications.

RNA base methylations in eukaryotes[19,20]. Emerging evidence demonstrates that m^{6}A deposition — catalysed by a writer complex comprising methyltransferase-like protein 3 (METTL3; also known as MTA70) and METTL14, Wilms tumour 1-associated protein (WTAP), protein virilizer homologue (KIAA1429), RNA-binding motif protein 15 (RBM15) and RBM15B[19–27] (FIG. 1b) — has important roles in regulating pre-mRNA processing. In mammals, m^{6}A is enriched in 3′ untranslated regions (3′ UTRs), introns and alternatively spliced exons[19,20,28]. Depletion of METTL3, WTAP or fat mass and obesity-associated protein (FTO), which is an m^{6}A eraser[29], results in splicing defects in hundreds of genes[19,26,30]. A portion of these events occurs in 3′ UTRs and final exons, which suggests that m^{6}A could also affect polyadenylation. Indeed, a higher m^{6}A density near proximal poly(A) sites correlates with a decreased use of those sites for polyadenylation, whereas the presence of m^{6}A near (and upstream to) distal poly(A) sites correlates with an increased use for polyadenylation in a subset of mRNAs[28].

A sizeable proportion (approximately 30%) of m^{6}A is found in introns, which indicates that these modifications are probably deposited co-transcriptionally and before splicing[24,31]. Similarly, the colocalization of m^{6}A writers and erasers with pre-mRNA splicing factors in the splicing-associated nuclear bodies known as speckles suggests an intrinsic connection between m^{6}A and splicing[24,32]. Furthermore, a deficiency of the m^{6}A demethylase alkB homologue 5 (ALKBH5) disrupts the recruitment of the splicing factors serine/arginine-rich splicing factor 1 (SRSF1), SRSF2 and SRSF protein kinase 1 (SRPK1) to nuclear speckles[32]. As the localization of SR proteins and their phosphorylation by SRPKs are intimately linked with splicing[33,34], these results may explain how changes in m^{6}A could affect global splice site choices. In another study, 60–80% of exonic FTO-regulated m^{6}A sites were found to overlap with exonic splicing-enhancer sequences that were bound by SRSF1 and SRSF2 (REF. 30). Strikingly, SRSF2 binding and exon inclusion are inversely correlated with FTO expression[32], which indicates that m^{6}A potentiates SRSF2 binding and splicing regulation. However, it is unclear whether SRSF2 binds m^{6}A directly or through m^{6}A-binding proteins. The m^{6}A reader YTH domain-containing protein 1 (YTHDC1) is an example that supports the second scenario. By binding to m^{6}A, YTHDC1 modulates thousands of splicing events through the promotion or inhibition of transcript binding by SRSF3 or SRSF10, respectively[35]. The *Drosophila melanogaster* homologue of YTHDC1, YT521-B, is also involved in splicing regulation. More than 100 splicing events are differentially regulated in the fly following knockdown of subunits of the m^{6}A writer complex[36,37]. Approximately 70% of these events are also misregulated upon depletion of YT521-B, indicating that this protein is the primary mediator of m^{6}A-dependent splicing regulation in *D. melanogaster*[37]. Notably, through binding to m^{6}A in the *Sex lethal* mRNA, YT521-B regulates sex determination by repressing the inclusion of the male-specific exon of the transcript[36,37]. Splicing factors can also bind directly to m^{6}A-containing sequences. A member of the heterogeneous

nuclear ribonucleoprotein (HNRNP) family of splicing factors, HNRNPA2B1, binds directly to METTL3-deposited m^{6}A-bearing regions near alternative exons and thereby affects their splicing[38]. Thus, m^{6}A serves as a docking site for proteins that can directly or indirectly influence pre-mRNA processing (FIG. 2).

Modifications and microRNAs cooperate to control mRNA decay. The development of chemical labelling techniques has led to the transcriptome-wide mapping of Ψ in yeast and human mRNAs[39–42]. Pseudouridylation of mRNAs is catalysed by the pseudouridine synthase (PUS) family of enzymes. Following heat shock in yeast, Pus7 catalyses Ψ formation at over 200 distinct sites in mRNAs[42]. The levels of Pus7 mRNA targets are higher than in Pus7-deficient cells, which suggests that Ψ actively regulates mRNA stability (FIG. 2). Conversely, depletion of the m^{6}A writer METTL3 results in a global increase in the half-life of METTL3 target mRNAs[43,44]. In mouse and human embryonic stem cells, this stabilization occurs in pluripotency genes, which results in a failure to exit the naive state of pluripotency[44,45]. These effects are regulated by the m^{6}A reader YTH domain family protein 2 (YTHDF2) and by the RBP human antigen R (HUR; also known as ELAVL1), with opposing consequences. YTHDF2 binding to m^{6}A recruits the CCR4–NOT deadenylase complex[46] and facilitates mRNA transport to processing bodies[47], which are sites of mRNA decay[48]. However, YTHDF2 was recently reported to stabilize HIV mRNAs and YTHDF2-tethered reporter constructs[49], which raises questions about the sole role of YTHDF2 in destabilizing mRNAs. By contrast, HUR stabilizes these mRNAs by binding to their 3′ UTRs and thereby blocks microRNA (miRNA) binding[31]. The decreased methylation that follows METTL3 depletion promotes HUR binding and stabilizes target transcripts by blocking miRNA-dependent mRNA decay.

The spatial proximity of m^{6}A and miRNA-binding sites in 3′ UTRs raises an interesting question: do miRNAs guide m^{6}A writers to specific adenosines? Recently, miRNAs were shown to modulate the binding of METTL3 to transcripts through a sequence-dependent pairing mechanism and to confer methylation specificity independently of the miRNA-interacting Argonaute (AGO) proteins[50]. Although intriguing, this result is yet to be validated by others. METTL3 also methylates many primary miRNAs (pri-miRNAs), which is obligatory for their processing by the Microprocessor complex subunit DiGeorge syndrome critical region 8 protein (DGCR8)[51]. This is mediated by HNRNPA2B1, which recruits DGCR8 to pri-miRNAs[51]. In addition, although the abundance of m^{5}C in mRNAs is low, transcriptome-wide profiling revealed substantial overlap between m^{5}C sites and AGO1–AGO4 binding sites[52], which suggests that m^{5}C might have a role in miRNA-mediated silencing. Recently, another modified nucleotide — *N*^{6},2′-O-dimethyladenosine (m^{6}A$_m$) — was found to be highly abundant adjacent to the 5′ cap of mRNAs in human cells[53]. m^{6}A$_m$ increases mRNA stability by conferring resistance to mRNA-decapping enzyme 2 (DCP2). As miRNA-mediated mRNA decay involves decapping, m^{6}A$_m$-modified mRNAs are more resistant to this mechanism of degradation[53]. Collectively, these studies highlight the dynamic cooperation between the epitranscriptome and miRNAs in modulating mRNA decay.

The epitranscriptome regulates translation under stress conditions. Translation regulation is a highly dynamic process that facilitates rapid responses to environmental stimuli, owing to the ample availability of translationally competent mRNA pools. Translation initiation can be cap-dependent or cap-independent[54], and the epitranscriptome has profound effects on both mechanisms.

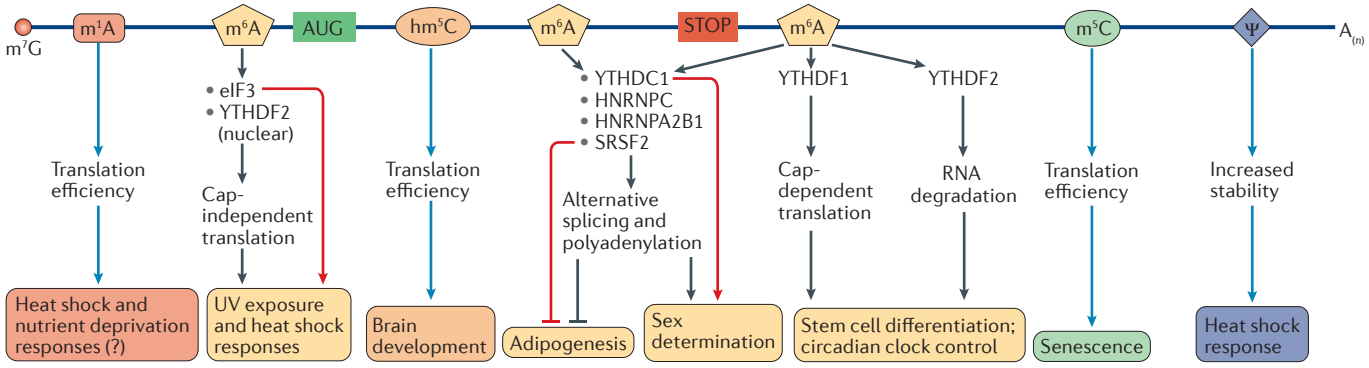

Figure 2 | **Biological functions of mRNA modifications.** The levels of *N*^{1}-methyladenosine (m^{1}A) and *N*^{6}-methyladenosine (m^{6}A) in 5′ untranslated regions (5′ UTRs) are dynamically altered in response to stress. m^{1}A promotes cap-dependent translation through an unknown reader. m^{1}A levels are altered by nutrient deprivation or heat shock, which indicates a possible role in directing cellular responses during these conditions (the question mark indicates that no direct link has been found). m^{6}A facilitates cap-independent translation through interactions with the eukaryotic translation initiation factor 3 (eIF3) complex in response to heat shock or UV exposure. YTH domain-containing family protein 2 (YTHDF2) protects 5′ UTR m^{6}A from demethylation. In coding sequences, 5-hydroxymethylcytosine (hm^{5}C) increases translation efficiency via an unknown mechanism; hm^{5}C levels are highest in the brain, and ablation of *Ten–eleven translocation* (*Tet*) genes, which encode proteins that catalyse hm^{5}C formation, affects brain development in *Drosophila melanogaster*. m^{6}A in coding regions affects RNA processing by modulating the binding of YTH domain-containing protein 1 (YTHDC1), heterogeneous nuclear ribonucleoprotein C (HNRNPC), HNRNPA2B1 and serine/arginine-rich splicing factor 2 (SRSF2). Removal of m^{6}A by fat mass and obesity-associated protein (FTO) (not shown) antagonizes SRSF2 binding and is necessary for adipogenesis. A homologue of YTHDC1, YT521-B, binds to m^{6}A in the *Sex lethal* mRNA and regulates its splicing, which in turn controls sex determination in *D. melanogaster*. m^{6}A in 3′ UTRs also affects RNA processing via the aforementioned readers, as well as cap-dependent translation via YTHDF1 and RNA degradation via YTHDF2. Regulation of mRNA stability by m^{6}A is crucial for stem cell differentiation and circadian clock control. 5-Methylcytosine (m^{5}C) is linked to the translational control of senescence-related genes. Pseudouridine (Ψ) in 3′ UTRs has been shown to increase the stability of modified transcripts during heat shock. Blue arrows indicate modifications with no known readers. Red lines connect readers to biological processes that they are directly associated with. A$_{(n)}$, polyadenylation; AUG, translation start codon; m^{7}G, 7-methylguanosine; STOP, translation stop codon.

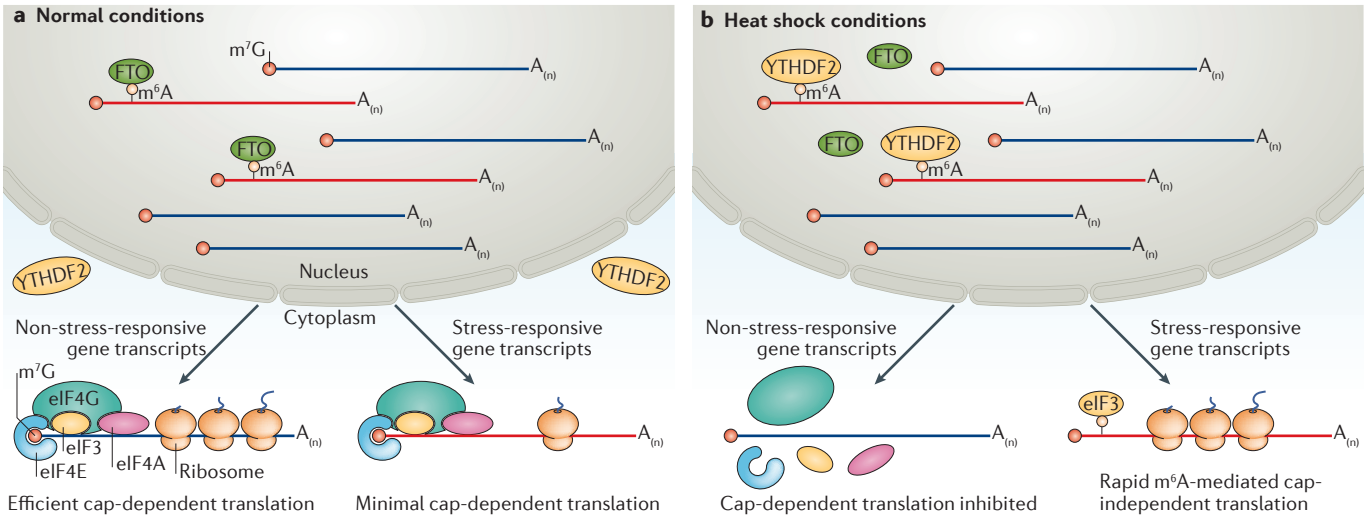

Figure 3 | **Stress induces *N*^{6}-methyladenosine-dependent translation.** Under normal conditions (part **a**), N^6-methyladenosine (m^6A) in the 5′ UTRs of stress-responsive gene transcripts is removed by the eraser fat mass and obesity-associated protein (FTO). Unmodified transcripts undergo efficient cap-dependent translation, whereas the demethylated transcripts of stress-responsive genes are minimally translated. Following heat shock (part **b**), the m^6A reader YTH domain-containing family protein 2 (YTHDF2) translocates from the cytoplasm to the nucleus, binds to m^6A in the 5′ UTR of stress-responsive mRNAs and prevents their FTO-mediated demethylation. Stress conditions globally inhibit cap-dependent translation of unmodified transcripts. However, the m^6A residues in the 5′ UTRs of stress responsive genes are directly bound by the eukaryotic translation initiation factor 3 (eIF3) complex, and this enables their rapid cap-independent translation. $A_{(n)}$, polyadenylation; m^7G, 7-methylguanosine.

In human cells, the m^6A reader YTHDF1 promotes cap-dependent translation initiation through its associations with the eukaryotic translation initiation factor 3 (eIF3) complex and other RBPs[55]. However, YTHDF1 has also been shown to regulate mRNA decay[46,49,56], which suggests that it has a role outside of translation. Although m^6A levels are low in 5′ UTRs, heat shock significantly increases m^6A levels specifically in the 5′ UTRs of heat shock-responsive mRNAs in mammalian cells in a YTHDF2-dependent manner[57,58]. Heat shock inhibits cap-dependent translation globally[59] but, remarkably, a single m^6A residue in a 5′ UTR is sufficient to facilitate cap-independent translation of heat shock-responsive mRNAs, which includes those encoding heat shock protein 70 kDa (HSP70)[57] (FIG. 3). Under normal conditions, FTO removes m^6A from the 5′ UTRs of HSP70 and other heat shock-responsive mRNAs, which prevents their cap-independent translation. During heat shock, YTHDF2 translocates from the cytoplasm to the nucleus and binds m^6A residues in the 5′ UTRs of heat shock-responsive mRNAs, which prevents demethylation by FTO and promotes rapid cap-independent translation[58]. In this way, 5′ UTR m^6A deposition ensures the production of proteins that are essential for survival during heat shock, even as general translation is halted.

m^5C and its derivative 5-hydroxymethylcytosine (hm^5C) are also implicated in translation regulation. Expression of the m^5C writer NOL1/NOP2/Sun domain family member 2 (NSUN2) is tightly regulated during the cell cycle, and the overexpression of NSUN2 delays replicative senescence through the methylation of cyclin-dependent kinase 1 (*CDK1*) and CDK inhibitor 1B (*CDKN1B*; which encodes p27) transcripts. Deposition of m^5C in the *CDK1* 3′ UTR enhances its translation, whereas m^5C in the 5′ UTR of *CDKN1B* represses its translation, which together result in increased cellular proliferation[60,61]. The formation of hm^5C from m^5C by methylcytosine dioxygenases[62] in mRNA correlates with an enhanced association with polyribosomes in *D. melanogaster*[63].

Recently, another modification, m^1A, was discovered[64,65]. Interestingly, m^1A displays plasticity in response to nitrogen deprivation in yeast[64], as well as tissue specificity and a rapid response to multiple stimuli in mammalian cells[64,65]. Most m^1A-modified transcripts harbour a single m^1A in their 5′ UTRs, and m^1A-bearing transcripts have higher translation efficiency and protein levels compared to unmodified transcripts. Finally, pseudouridylation can affect the translation of some transcripts by alternative decoding of pseudouridylated codons, which may improve stress tolerance[66].

Although somewhat preliminary, these studies demonstrate the effects of RNA modifications on different steps of gene expression, which raises the question of how the modifications link various nuclear and cytosolic processes. For example, in the case of m^6A, the discrete cellular localization of readers and their distinct protein interaction domains seem to allow their interaction with different effectors to regulate specific processes in the nucleus and cytoplasm[30,35,38,47,55,58].

RNA structure

Unlike DNA, which universally adopts a double helical conformation, RNA has extensive intramolecular interactions that cause it to fold into an array of complex structures[67]. RNA structure is highly dynamic and is governed by factors such as temperature, cellular energy state, ATP-dependent RNA helicases, chaperone proteins and other RBPs[68]. RNA structures enable a myriad of functions, which include encoding genetic information and catalysing chemical reactions[69,70]. The dynamic nature of RNA structure is illustrated by splicing, during which structural rearrangements of snRNAs permit the recognition of splice sites and branch point sequences in pre-mRNAs and facilitate the stepwise assembly of spliceosomes[71]. Numerous studies have confirmed that mRNAs also contain

structured regions, although the extent of folding is significantly lower than that of non-coding RNAs. The advent of chemical modification-based procedures and RBP–RNA crosslinking methods[11,12,72,73] have enabled transcriptome-wide mapping of RNA structures in different species. These studies have unveiled a previously unappreciated and complex layer of gene regulation.

RNA structures shape protein binding and splicing. RNA folding begins as the transcript is synthesized by RNA polymerase II (Pol II)[74–76]. Transcript elongation by Pol II is not continuous, but instead entails periods of active elongation that are interrupted by pauses and backtracking. The formation of RNA structures such as hairpins on the nascent transcript can create physical barriers that prevent backtracking and promote forward elongation by Pol II[74,75]. As splicing and polyadenylation are dependent on Pol II elongation kinetics[77,78], the effect of RNA structure on transcript elongation probably affects downstream RNA processing.

RNA structures may also regulate RNA processing directly by three distinct mechanisms. First, local RNA structure variations can promote or inhibit the binding of RBPs[8]. For example, secondary structures surrounding the consensus motifs for the splicing factors RBP FOX-1 homologue 2 (RBFOX2) and muscleblind-like protein 1 (MBNL1) are key determinants of whether these sites will be bound *in vivo*. Furthermore, motifs near evolutionarily conserved alternative exons tend to be more single-stranded and to exhibit stronger RBP binding than species-specific alternative exons or constitutive exons[8]. Distinct structural features also occur at 5′ and 3′ splice sites, at strong and weak splice sites and at polyadenylation signals, which indicates that local structures regulate RNA processing globally[72,79,80].

Second, larger RNA structures can regulate splicing by bringing distal regulatory elements in close proximity to target exons. For example, more than half of the RBFOX2-binding sites are found over 500 nucleotides away from any annotated exon[81]. Regulation from these deep intronic sites occurs by the formation of long-range intronic structures that deliver RBFOX2 close to its target exons (FIG. 4a). Moreover, recent studies utilizing methods that detect large RNA duplexes have revealed that up to 40% of transcript structures span more than 300 nucleotides[10,82,83]. Thus, the RNA structure-based proximity system observed for RBFOX2 may represent a mechanism that is common to other RBPs.

Third, RNA modifications may act to stabilize or disrupt structural elements and influence RBP accessibility. This mechanism has been shown to regulate the binding of HNRNPC[84], an RBP that is involved in mRNA stability and processing[7,85,86]. The U-tract sequences that are recognized by HNRNPC are often buried within stem structures, which prevent HNRNPC binding. Adenosines in these stems are often N^6-methylated, which destabilizes the stem structure to expose the U-tract and allow binding by HNRNPC (FIG. 4b). Thousands of such m^{6}A structural switches have been identified, and the expression of nearly 2,000 genes and more than 100 splicing events are regulated by HNRNPC and METTL3–METTL14 (REF. 84). Taken together, these studies indicate that the

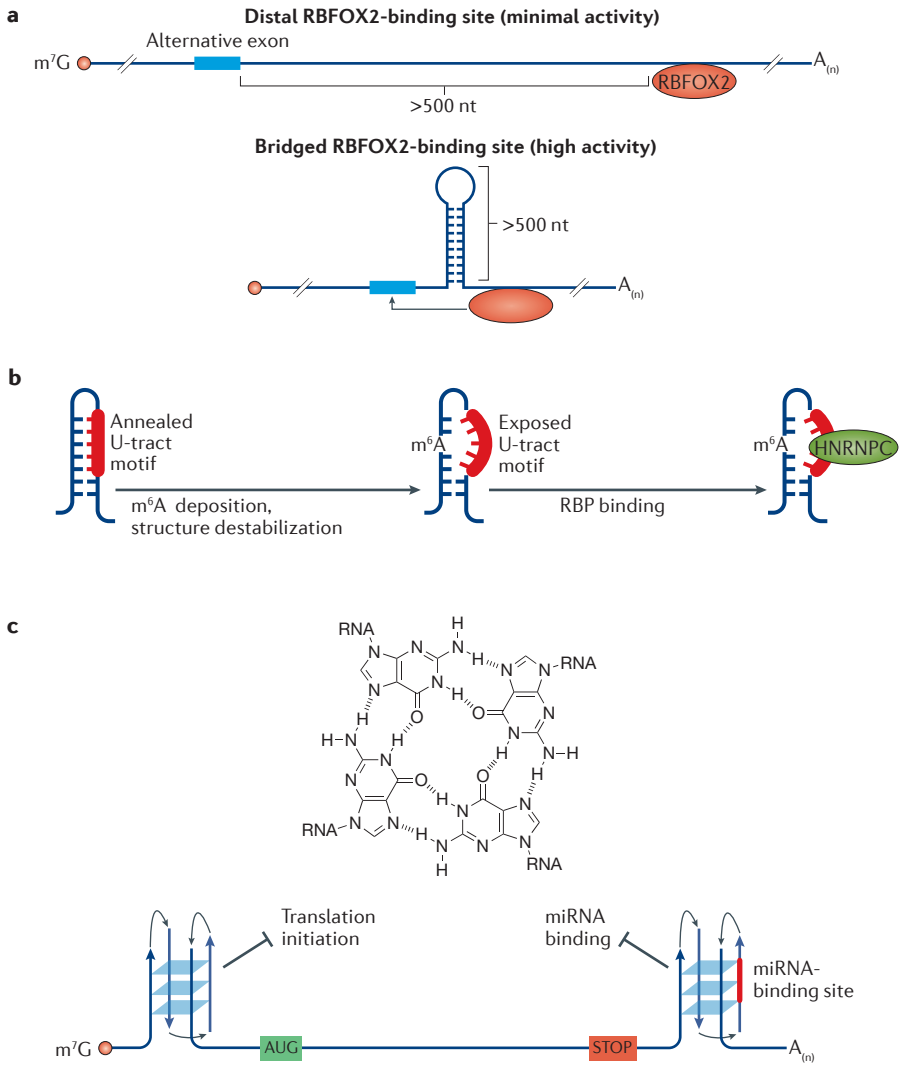

Figure 4 | **The effect of RNA structures on mRNA modification and gene expression. a** | A majority of RNA-binding protein FOX-1 homologue 2 (RBFOX2) binding sites are over 500 nucleotides (nt) away from the nearest exon. To enable splicing regulation by RBFOX2 from these distal binding sites, base-pairing interactions occur within the intron, which bring RBFOX2 into close proximity to its target exons. **b** | N^6-methyladenosine (m^{6}A) deposition destabilizes base-pairing interactions and disrupts local secondary structures. In doing so, m^{6}A can expose previously buried RNA-binding motifs to RNA-binding proteins (RBPs), such as the U-tracts that are bound by heterogeneous nuclear ribonucleoprotein C (HNRNPC). **c** | RNA G-quadruplexes (RGQs) form by the stacking of three or more guanine quartets (top panel). In 5′ untranslated regions (5′ UTRs), RGQs impede the initiation and scanning steps of translation (bottom panel). In 3′ UTRs, RGQs can block access to microRNA (miRNA)-binding sites and thus prevent miRNA-mediated decay and translation repression. RGQs are dynamic structures and can be unwound by RNA helicases. $A_{(n)}$, polyadenylation; AUG, translation start codon; m^{7}G, 7-methylguanosine; STOP, translation stop codon. Part **b** is adapted with permission from REF. 84, Macmillan Publishers Ltd.

structural landscape of the transcriptome is an essential mediator of RNA processing and is yet another factor that must be fully understood to complete the splicing code.

RNA structures tune translation and mRNA stability. RNA structure has also been linked to translation regulation. In plants, animals and fungi, the approximately five-nucleotide region surrounding the start codon displays a remarkable lack of structure[11,72,80,87,88]. This feature is enriched in genes with high translation efficiency and is absent in those with low efficiency[11,72,80,87,88], which indicates that start codon accessibility promotes translation. RNA secondary structure is also highly dynamic in response to external stimuli. In yeast, following the transition from 30 °C to 37 °C, base-pairing of over 25,000 bases at approximately 2,000 structured sites in mRNAs is disrupted[88]. These heat-sensitive bases are enriched in 5′ UTRs, regions in which structure is known to influence translation[89].

Another structural element that has gained attention in the past decade is the RNA G-quadruplex (RGQ), which is a four-stranded structure that results from the stacking of multiple planar guanine quartets (FIG. 4c). RGQs are implicated in splicing, transcript stability and translation regulation. Although they are prevalent *in vitro* — especially in 5′ and 3′ UTRs — recent *in vivo* genome-wide analysis has revealed that RGQs are globally unfolded in mammalian cells[90]. Nonetheless, many individual examples of functionally important RGQs exist[89,91]. In T cell acute lymphoblastic leukaemia cells, inhibition of the RGQ-helicase eukaryotic translation initiation factor 4A1 (eIF4A1) induces apoptosis and delays tumour growth owing to decreased translation of oncogenes such as myelocytomatosis proto-oncogene (*MYC*), *Notch*, and *BCL-2* (REF. 92). Transcripts affected by eIF4A1 inhibition have longer 5′ UTRs on average and display a strong enrichment for the twelve-nucleotide RGQ-forming motif $(CGG)_4$. Thus, the tumorigenic properties of eIF4A1 may be based on its ability to unwind translation-inhibiting RGQs in the 5′ UTRs of oncogenes. In addition to 5′ structures, RGQs in the 3′ UTRs of mRNAs can also affect mRNA translation and stability through the occlusion of miRNA-binding sites[93] (FIG. 4c).

The degradation of mRNAs is primarily controlled by the exosome, which is a multiprotein exonuclease[94]. Exosome-mediated degradation requires a single-stranded region at the 3′ end of mRNAs, which potentially enables RNA structures to affect transcript stability. Indeed, 3′ UTR structures that involve the poly(A) tail are the primary determinants of transcript stability in yeast and result in alternative polyadenylation isoforms with drastically different stabilities[95,96], although stability differences between such 3′ UTR isoforms are subtler in mammalian cells[97]. Interestingly, a sizeable portion (15–25%) of annotated mRNAs and long non-coding RNAs (lncRNAs) are not polyadenylated or are bimorphic, so that some transcripts contain and others lack a poly(A) tail[98], which raises the question of how these transcripts are stabilized and, in the case of mRNAs, translated. The intronless, replication-dependent histones are one such group of non-polyadenylated mRNAs. These mRNAs are instead stabilized by highly conserved stem-loop structures that form in their 3′ UTRs, which are also required for their translation[99]. Furthermore, additional 3′ structures (such as triple helices) can also stabilize mRNAs and lncRNAs.

RNA triple helices are structures that result when an RNA strand forms Hoogsteen hydrogen bonds with the major groove of an RNA duplex. The triple helix structure that forms at the expression and nuclear retention element (ENE) in the 3′ end of the Kaposi sarcoma-associated herpesvirus lncRNA, polyadenylated nuclear RNA (PAN RNA), protects the transcript from rapid nuclear deadenylation-dependent decay[100–102]. Recently, a pair of studies discovered similar ENEs in two mammalian non-polyadenylated lncRNAs, metastasis-associated lung adenocarcinoma transcript 1 (MALAT1) and multiple endocrine neoplasia-β (MENβ; also known as NEAT1)[103,104]. Both MALAT1 and MENβ are not processed by the canonical cleavage and polyadenylation machinery, and instead they contain tRNA-like structures in their 3′ ends that are cleaved by RNase P[105,106]. Following cleavage, genomically encoded A-rich tracts at the 3′ ends of both lncRNAs form triple helices, which are nearly identical to those formed in the PAN RNA[103,104]. These structures are essential for the stability of MALAT1 and MENβ, as shown by deletions of or destabilizing mutations in these structures. Strikingly, placement of the MALAT1 and MENβ 3′ structures into polyadenylation-deficient reporter genes not only significantly stabilizes mRNAs but also facilitates efficient translation[104], suggesting that such RNA structures may have a wider

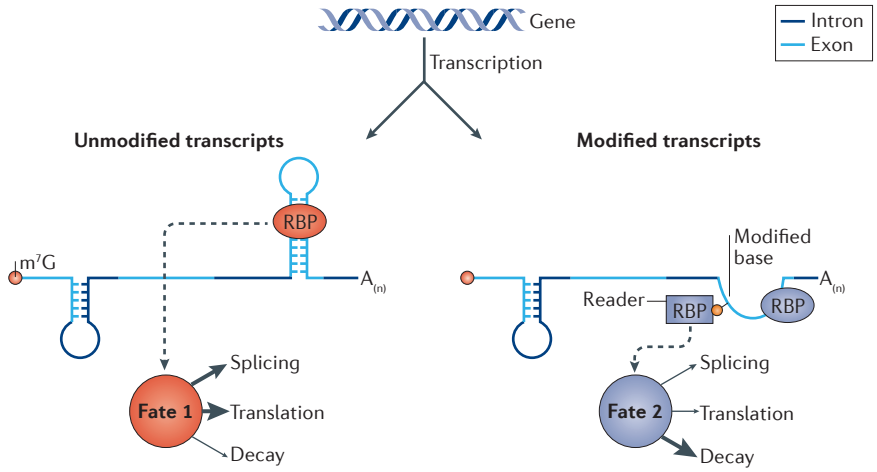

Cell state 1	90%	10%
Cell state 2	30%	70%

Figure 5 | **The dynamics of mRNA modification stoichiometries.** Within the pool of transcripts from a given gene, each potential modification site is modified in only a fraction of transcripts, which is known as the modification stoichiometry. The modification stoichiometry may be very low under certain cellular conditions (cell state 1). By causing RNA structural rearrangements and directly recruiting modification reader proteins, the modified mRNAs acquire a different fate, which could result, for example, in increased turnover (decay). As cellular conditions change, modification stoichiometry may change as well, which can result in a higher (cell state 2) or lower percentage of modified transcripts owing to alterations in reader, writer and/or eraser activity or expression. The dashed arrows indicate an indirect effect. $A_{(n)}$, polyadenylation; m^7G, 7-methylguanosine; RBP, RNA-binding protein.

role in the translation and/or stabilization of other poly(A)-lacking transcripts. Recently, bioinformatics analysis identified similar structures that stabilize hundreds of transposon transcripts in fungi, providing the first evidence of the existence of triple helices in mRNAs[107].

During heat shock in yeast, RNA structures with low melting temperatures are rapidly degraded by the exosome as their 3′ ends become accessible[88]. As discussed above, Ψ deposition increases following heat shock, which increases mRNA stability[42]. As Ψ-A base pairs are more stable than U-A base pairs[66], it is possible that Ψ increases mRNA stability by preventing the melting of RNA structures that protect the 3′ end at increased temperatures. In contrast to Ψ, m^{6}A acts as a 'spring-loaded' modification, which disrupts RNA duplexes owing to the adoption of an unfavourable, high-energy conformation[108,109]. Indeed, transcriptome-wide structure analysis revealed a distinct structural profile at m^{6}A sites, which is consistent with unpaired RNA[11]. Besides its role in miRNA-mediated decay, the strong enrichment of m^{6}A in 3′ UTRs suggests that it may also promote transcript degradation by destabilizing 3′-protecting structural elements. Interestingly, 3′ UTR structures are not always protective. Transcriptome-wide analysis of Staufen homologue 1 (STAU1), which binds double-stranded RNA and regulates mRNA stability[110], revealed that it binds to thousands of duplexes in 3′ UTRs[12]. Depletion of STAU1 significantly increased the stability of mRNAs containing these 3′ duplexes, demonstrating that these structures promote mRNA degradation.

Future perspectives

An increasing body of evidence shows that dynamic changes in RNA structures and modifications are indispensable features of eukaryotic gene expression and supports a new paradigm in which these features promote the coordination of gene expression processes by modulating the access of specific RBPs and facilitating active transcriptome reprogramming in response to varying cellular conditions. Current RNA structural data represent only brief snapshots in time. However, it is likely that mRNAs are dynamically refolded as they progress through their life cycle, enter distinct subcellular compartments and associate with different RBPs. These structural rearrangements may affect downstream processes and facilitate the remodelling of the mRNA–protein complex through the occlusion, exposure or formation of RBP-binding sites. Thus, the tracking of individual transcript structures throughout their life cycle will be necessary to fully understand the impact of mRNA structure on gene expression. Future studies should discern how external cues fine-tune the structural and chemical variations within transcript pools to produce a coherent biological response. For example, do different signalling pathways recruit discrete epitranscriptome readers, writers or erasers as effectors to influence the fates of individual mRNAs? Efforts to map the epitranscriptome at single-nucleotide resolution must also continue in order to identify the exact nucleotides that are modified in each transcript, define how these sites are selected and determine whether these dynamics are achieved through the active control of writers versus erasers.

Another important aspect that is yet to be addressed is the dynamics of RNA modification stoichiometry. Current epitranscriptome studies deal mostly with identifying which sites are modified and not the fraction of RNAs in which each site is modified. Low-throughput analysis of m^{6}A modification sites in mRNA and viral RNA shows that no m^{6}A site is modified in 100% of transcripts[111–113]. Changes in modification stoichiometry may also represent a dynamic parameter of RNA modification biology. As modifications can affect mRNA structure and/or the recruitment of RBPs, modification of a fraction of transcripts at any specific site would generate two distinct mRNA species that differ only in their structures or the readers that bind to them (FIG. 5). Therefore, changing modification stoichiometry could represent another mechanism to generate functional diversity from the same RNA transcript. High-throughput methods that can determine modification stoichiometry are needed to address this aspect of the epitranscriptome. This is especially important for identifying the functional modifications in heavily modified transcripts. For example, nearly 80 distinct sites in the lncRNA X-inactive specific transcript (*XIST*) are m^{6}A — more than any other RNA — and modification of *XIST* is necessary for recruiting YTHDC1 and for the transcriptional silencing of genes on the X chromosome[25]. However, the percentage of adenosines that are modified and, in turn, which modified bases or combinations of modified bases are required for X-chromosome inactivation, is unknown.

Finally, we also need to further explore how structural and chemical alterations cooperate to allow the functional coupling of the different steps of the mRNA life cycle. In addition to the functions provided by direct readers, RNA modifications may be one of the primary drivers of structural plasticity within the transcriptome by stabilizing or disrupting base-pairing interactions. As such, the phenotypes observed following perturbation of the activity of writers or erasers may partially be the result of global changes in the RNA structural topography.

Cole J.T. Lewis and Auinash Kalsotra are at the Department of Biochemistry, University of Illinois; A.K. is also at the Institute of Genomic Biology, University of Illinois, Urbana-Champaign, Illinois 61801, USA.

Tao Pan is at the Department of Biochemistry and Molecular Biology, University of Chicago, Chicago, Illinois 60637, USA.

Correspondence to T.P. and A.K.
taopan@uchicago.edu; kalsotra@illinois.edu

doi:10.1038/nrm.2016.163
Published online 1 Feb 2017

1. Howard, J. M. & Sanford, J. R. The RNAissance family: SR proteins as multifaceted regulators of gene expression. *Wiley Interdiscip. Rev. RNA* **6**, 93–110 (2015).
2. Huang, Y., Gattoni, R., Stevenin, J. & Steitz, J. A. SR splicing factors serve as adapter proteins for TAP-dependent mRNA export. *Mol. Cell* **11**, 837–843 (2003).
3. Muller-McNicoll, M. *et al.* SR proteins are NXF1 adaptors that link alternative RNA processing to mRNA export. *Genes Dev.* **30**, 553–566 (2016).
4. Ji, X. *et al.* SR proteins collaborate with 7SK and promoter-associated nascent RNA to release paused polymerase. *Cell* **153**, 855–868 (2013).
5. Singh, G. *et al.* The cellular EJC interactome reveals higher-order mRNP structure and an EJC-SR protein nexus. *Cell* **151**, 750–764 (2012).
6. Hafner, M. *et al.* Transcriptome-wide identification of RNA-binding protein and microRNA target sites by PAR-CLIP. *Cell* **141**, 129–141 (2010).
7. Konig, J. *et al.* iCLIP reveals the function of hnRNP particles in splicing at individual nucleotide resolution. *Nat. Struct. Mol. Biol.* **17**, 909–915 (2010).
8. Taliaferro, J. M. *et al.* RNA sequence context effects measured in vitro predict *in vivo* protein binding and regulation. *Mol. Cell* **64**, 294–306 (2016).
9. Gilbert, W. V., Bell, T. A. & Schaening, C. Messenger RNA modifications: form, distribution, and function. *Science* **352**, 1408–1412 (2016).
10. Lu, Z. *et al.* RNA duplex map in living cells reveals higher-order transcriptome structure. *Cell* **165**, 1267–1279 (2016).
11. Spitale, R. C. *et al.* Structural imprints *in vivo* decode RNA regulatory mechanisms. *Nature* **519**, 486–490 (2015).
12. Sugimoto, Y. *et al.* hiCLIP reveals the *in vivo* atlas of mRNA secondary structures recognized by Staufen 1. *Nature* **519**, 491–494 (2015).
13. Nishikura, K. A-To-I editing of coding and non-coding RNAs by ADARs. *Nat. Rev. Mol. Cell Biol.* **17**, 83–96 (2016).
14. Blanc, V. & Davidson, N. O. APOBEC-1-mediated RNA editing. *Wiley Interdiscip. Rev. Syst. Biol. Med.* **2**, 594–602 (2010).
15. Cantara, W. A. *et al.* The RNA Modification Database, RNAMDB: 2011 update. *Nucleic Acids Res.* **39**, D195–D201 (2011).
16. El Yacoubi, B., Bailly, M. & de Crecy-Lagard, V. Biosynthesis and function of posttranscriptional modifications of transfer RNAs. *Annu. Rev. Genet.* **46**, 69–95 (2012).

17. Karijolich, J., Kantartzis, A. & Yu, Y. T. RNA modifications: a mechanism that modulates gene expression. *Methods Mol. Biol.* **629**, 1–19 (2010).
18. Barash, Y. *et al.* Deciphering the splicing code. *Nature* **465**, 53–59 (2010).
19. Dominissini, D. *et al.* Topology of the human and mouse m^{6}A RNA methylomes revealed by m^{6}A-seq. *Nature* **485**, 201–206 (2012).
20. Meyer, K. D. *et al.* Comprehensive analysis of mRNA methylation reveals enrichment in 3′ UTRs and near stop codons. *Cell* **149**, 1635–1646 (2012).
21. Schwartz, S. *et al.* Perturbation of m^{6}A writers reveals two distinct classes of mRNA methylation at internal and 5′ sites. *Cell Rep.* **8**, 284–296 (2014).
22. Agarwala, S. D., Blitzblau, H. G., Hochwagen, A. & Fink, G. R. RNA methylation by the MIS complex regulates a cell fate decision in yeast. *PLoS Genet.* **8**, e1002732 (2012).
23. Horiuchi, K. *et al.* Identification of Wilms' tumor 1-associating protein complex and its role in alternative splicing and the cell cycle. *J. Biol. Chem.* **288**, 33292–33302 (2013).
24. Liu, J. *et al.* A METTL3–METTL14 complex mediates mammalian nuclear RNA *N*^{6}-adenosine methylation. *Nat. Chem. Biol.* **10**, 93–95 (2014).
25. Patil, D. P. *et al.* m^{6}A RNA methylation promotes *XIST*-mediated transcriptional repression. *Nature* **537**, 369–373 (2016).
26. Ping, X. L. *et al.* Mammalian WTAP is a regulatory subunit of the RNA *N*^{6}-methyladenosine methyltransferase. *Cell Res.* **24**, 177–189 (2014).
27. Zhong, S. *et al.* MTA is an *Arabidopsis* messenger RNA adenosine methylase and interacts with a homolog of a sex-specific splicing factor. *Plant Cell* **20**, 1278–1288 (2008).
28. Ke, S. *et al.* A majority of m^{6}A residues are in the last exons, allowing the potential for 3′ UTR regulation. *Genes Dev.* **29**, 2037–2053 (2015).
29. Jia, G. *et al.* *N*^{6}-methyladenosine in nuclear RNA is a major substrate of the obesity-associated FTO. *Nat. Chem. Biol.* **7**, 885–887 (2011).
30. Zhao, X. *et al.* FTO-dependent demethylation of *N*^{6}-methyladenosine regulates mRNA splicing and is required for adipogenesis. *Cell Res.* **24**, 1403–1419 (2014).
31. Wang, Y. *et al.* *N*^{6}-methyladenosine modification destabilizes developmental regulators in embryonic stem cells. *Nat. Cell Biol.* **16**, 191–198 (2014).
32. Zheng, G. *et al.* ALKBH5 is a mammalian RNA demethylase that impacts RNA metabolism and mouse fertility. *Mol. Cell* **49**, 18–29 (2013).
33. Zhong, X. Y., Ding, J. H., Adams, J. A., Ghosh, G. & Fu, X. D. Regulation of SR protein phosphorylation and alternative splicing by modulating kinetic interactions of SRPK1 with molecular chaperones. *Genes Dev.* **23**, 482–495 (2009).
34. Zhong, X. Y., Wang, P., Han, J., Rosenfeld, M. G. & Fu, X. D. SR proteins in vertical integration of gene expression from transcription to RNA processing to translation. *Mol. Cell* **35**, 1–10 (2009).
35. Xiao, W. *et al.* Nuclear m^{6}A reader YTHDC1 regulates mRNA splicing. *Mol. Cell* **61**, 507–519 (2016).
36. Haussmann, I.U. *et al.* m6A potentiates Sxl alternative pre-mRNA splicing for robust Drosophila sex determination. *Nature* **540**, 301–304 (2016).
37. Lence, T. *et al.* m6A modulates neuronal functions and sex determination in Drosophila. *Nature* **540**, 242–247 (2016).
38. Alarcon, C. R. *et al.* HNRNPA2B1 is a mediator of m^{6}A-dependent nuclear RNA processing events. *Cell* **162**, 1299–1308 (2015).
39. Carlile, T. M. *et al.* Pseudouridine profiling reveals regulated mRNA pseudouridylation in yeast and human cells. *Nature* **515**, 143–146 (2014).
40. Li, X. *et al.* Chemical pulldown reveals dynamic pseudouridylation of the mammalian transcriptome. *Nat. Chem. Biol.* **11**, 592–597 (2015).
41. Lovejoy, A. F., Riordan, D. P. & Brown, P. O. Transcriptome-wide mapping of pseudouridines: pseudouridine synthases modify specific mRNAs in *S. cerevisiae*. *PLoS ONE* **9**, e110799 (2014).
42. Schwartz, S. *et al.* Transcriptome-wide mapping reveals widespread dynamic-regulated pseudouridylation of ncRNA and mRNA. *Cell* **159**, 148–162 (2014).
43. Sommer, S., Lavi, U. & Darnell, J. E. Jr. The absolute frequency of labeled *N*-6-methyladenosine in HeLa cell messenger RNA decreases with label time. *J. Mol. Biol.* **124**, 487–499 (1978).
44. Batista, P. J. *et al.* m^{6}A RNA modification controls cell fate transition in mammalian embryonic stem cells. *Cell Stem Cell* **15**, 707–719 (2014).
45. Geula, S. *et al.* Stem cells. m^{6}A mRNA methylation facilitates resolution of naive pluripotency toward differentiation. *Science* **347**, 1002–1006 (2015).
46. Du, H. *et al.* YTHDF2 destabilizes m^{6}A-containing RNA through direct recruitment of the CCR4–NOT deadenylase complex. *Nat. Commun.* **7**, 12626 (2016).
47. Wang, X. *et al.* *N*^{6}-methyladenosine-dependent regulation of messenger RNA stability. *Nature* **505**, 117–120 (2014).
48. Sheth, U. & Parker, R. Decapping and decay of messenger RNA occur in cytoplasmic processing bodies. *Science* **300**, 805–808 (2003).
49. Kennedy, E. M. *et al.* Posttranscriptional m^{6}A editing of HIV-1 mRNAs enhances viral gene expression. *Cell Host Microbe* **19**, 675–685 (2016).
50. Chen, T. *et al.* m^{6}A RNA methylation is regulated by microRNAs and promotes reprogramming to pluripotency. *Cell Stem Cell* **16**, 289–301 (2015).
51. Alarcon, C. R., Lee, H., Goodarzi, H., Halberg, N. & Tavazoie, S. F. *N*^{6}-methyladenosine marks primary microRNAs for processing. *Nature* **519**, 482–485 (2015).
52. Squires, J. E. *et al.* Widespread occurrence of 5-methylcytosine in human coding and non-coding RNA. *Nucleic Acids Res.* **40**, 5023–5033 (2012).
53. Mauer, J. *et al.* Reversible methylation of m6Am in the 5′ cap controls mRNA stability. *Nature* http://dx.doi.org/10.1038/nature21022 (2016).
54. Merrick, W. C. Cap-dependent and cap-independent translation in eukaryotic systems. *Gene* **332**, 1–11 (2004).
55. Wang, X. *et al.* *N*^{6}-methyladenosine modulates messenger RNA translation efficiency. *Cell* **161**, 1388–1399 (2015).
56. Tirumuru, N. *et al.* *N*^{6}-methyladenosine of HIV-1 RNA regulates viral infection and HIV-1 Gag protein expression. *Elife* **5** e15528 (2016).
57. Meyer, K. D. *et al.* 5′ UTR m^{6}A promotes cap-independent translation. *Cell* **163**, 999–1010 (2015).
58. Zhou, J. *et al.* Dynamic m^{6}A mRNA methylation directs translational control of heat shock response. *Nature* **526**, 591–594 (2015).
59. Feigenblum, D. & Schneider, R. J. Cap-binding protein (eukaryotic initiation factor 4E) and 4E-inactivating protein BP-1 independently regulate cap-dependent translation. *Mol. Cell. Biol.* **16**, 5450–5457 (1996).
60. Tang, H. *et al.* NSun2 delays replicative senescence by repressing p27^{KIP1} translation and elevating CDK1 translation. *Aging (Albany NY)* **7**, 1143–1158 (2015).
61. Xing, J. *et al.* NSun2 promotes cell growth via elevating cyclin-dependent kinase 1 translation. *Mol. Cell. Biol.* **35**, 4043–4052 (2015).
62. Fu, L. *et al.* Tet-mediated formation of 5-hydroxymethylcytosine in RNA. *J. Am. Chem. Soc.* **136**, 11582–11585 (2014).
63. Delatte, B. *et al.* RNA biochemistry. Transcriptome-wide distribution and function of RNA hydroxymethylcytosine. *Science* **351**, 282–285 (2016).
64. Dominissini, D. *et al.* The dynamic *N*^{1}-methyladenosine methylome in eukaryotic messenger RNA. *Nature* **530**, 441–446 (2016).
65. Li, X. *et al.* Transcriptome-wide mapping reveals reversible and dynamic *N*^{1}-methyladenosine methylome. *Nat. Chem. Biol.* **12**, 311–316 (2016).
66. Karijolich, J., Yi, C. & Yu, Y. T. Transcriptome-wide dynamics of RNA pseudouridylation. *Nat. Rev. Mol. Cell Biol.* **16**, 581–585 (2015).
67. Wan, Y., Kertesz, M., Spitale, R. C., Segal, E. & Chang, H. Y. Understanding the transcriptome through RNA structure. *Nat. Rev. Genet.* **12**, 641–655 (2011).
68. Dethoff, E. A., Chugh, J., Mustoe, A. M. & Al-Hashimi, H. M. Functional complexity and regulation through RNA dynamics. *Nature* **482**, 322–330 (2012).
69. Cech, T. R. & Steitz, J. A. The noncoding RNA revolution — trashing old rules to forge new ones. *Cell* **157**, 77–94 (2014).
70. Sharp, P. A. The centrality of RNA. *Cell* **136**, 577–580 (2009).
71. Smith, D. J., Query, C. C. & Konarska, M. M. "Nought may endure but mutability": spliceosome dynamics and the regulation of splicing. *Mol. Cell* **30**, 657–666 (2008).
72. Ding, Y. *et al.* *In vivo* genome-wide profiling of RNA secondary structure reveals novel regulatory features. *Nature* **505**, 696–700 (2014).
73. Rouskin, S., Zubradt, M., Washietl, S., Kellis, M. & Weissman, J. S. Genome-wide probing of RNA structure reveals active unfolding of mRNA structures *in vivo*. *Nature* **505**, 701–705 (2014).
74. Liu, S. R., Hu, C. G. & Zhang, J. Z. Regulatory effects of cotranscriptional RNA structure formation and transitions. *Wiley Interdiscip. Rev. RNA* **7**, 562–574 (2016).
75. Zhang, J. & Landick, R. A. Two-way street: regulatory interplay between RNA polymerase and nascent RNA structure. *Trends Biochem. Sci.* **41**, 293–310 (2016).
76. Pan, T. & Sosnick, T. RNA folding during transcription. *Annu. Rev. Biophys. Biomol. Struct.* **35**, 161–175 (2006).
77. de la Mata, M. *et al.* A slow RNA polymerase II affects alternative splicing *in vivo*. *Mol. Cell* **12**, 525–532 (2003).
78. Pinto, P. A. *et al.* RNA polymerase II kinetics in polo polyadenylation signal selection. *EMBO J.* **30**, 2431–2444 (2011).
79. Jin, Y., Yang, Y. & Zhang, P. New insights into RNA secondary structure in the alternative splicing of pre-mRNAs. *RNA Biol.* **8**, 450–457 (2011).
80. Wan, Y. *et al.* Landscape and variation of RNA secondary structure across the human transcriptome. *Nature* **505**, 706–709 (2014).
81. Lovci, M. T. *et al.* Rbfox proteins regulate alternative mRNA splicing through evolutionarily conserved RNA bridges. *Nat. Struct. Mol. Biol.* **20**, 1434–1442 (2013).
82. Aw, J. G. *et al.* *In vivo* mapping of eukaryotic RNA interactomes reveals principles of higher-order organization and regulation. *Mol. Cell* **62**, 603–617 (2016).
83. Sharma, E., Sterne-Weiler, T., O'Hanlon, D. & Blencowe, B. J. Global mapping of human RNA–RNA interactions. *Mol. Cell* **62**, 618–626 (2016).
84. Liu, N. *et al.* *N*^{6}-methyladenosine-dependent RNA structural switches regulate RNA-protein interactions. *Nature* **518**, 560–564 (2015).
85. McCloskey, A., Taniguchi, I., Shinmyozu, K. & Ohno, M. hnRNP C tetramer measures RNA length to classify RNA polymerase II transcripts for export. *Science* **335**, 1643–1646 (2012).
86. Zarnack, K. *et al.* Direct competition between hnRNP C and U2AF65 protects the transcriptome from the exonization of Alu elements. *Cell* **152**, 453–466 (2013).
87. Kertesz, M. *et al.* Genome-wide measurement of RNA secondary structure in yeast. *Nature* **467**, 103–107 (2010).
88. Wan, Y. *et al.* Genome-wide measurement of RNA folding energies. *Mol. Cell* **48**, 169–181 (2012).
89. Bugaut, A. & Balasubramanian, S. 5′-UTR RNA G-quadruplexes: translation regulation and targeting. *Nucleic Acids Res.* **40**, 4727–4741 (2012).
90. Guo, J. U. & Bartel, D. P. RNA G-quadruplexes are globally unfolded in eukaryotic cells and depleted in bacteria. *Science* **353** (2016).
91. Millevoi, S., Moine, H. & Vagner, S. G-Quadruplexes in RNA biology. *Wiley Interdiscip. Rev. RNA* **3**, 495–507 (2012).
92. Wolfe, A. L. *et al.* RNA G-quadruplexes cause eIF4A-dependent oncogene translation in cancer. *Nature* **513**, 65–70 (2014).
93. Kenny, P. J. *et al.* MOV10 and FMRP regulate AGO2 association with microRNA recognition elements. *Cell Rep.* **9**, 1729–1741 (2014).
94. Houseley, J., LaCava, J. & Tollervey, D. RNA-quality control by the exosome. *Nat. Rev. Mol. Cell Biol.* **7**, 529–539 (2006).
95. Geisberg, J. V., Moqtaderi, Z., Fan, X., Ozsolak, F. & Struhl, K. Global analysis of mRNA isoform half-lives reveals stabilizing and destabilizing elements in yeast. *Cell* **156**, 812–824 (2014).
96. Moqtaderi, Z., Geisberg, J. V. & Struhl, K. Secondary structures involving the poly(A) tail and other 3′ sequences are major determinants of mRNA isoform stability in yeast. *Microb. Cell* **1**, 137–139 (2014).
97. Spies, N., Burge, C. B. & Bartel, D. P. 3′ UTR-isoform choice has limited influence on the stability and translational efficiency of most mRNAs in mouse fibroblasts. *Genome Res.* **23**, 2078–2090 (2013).
98. Yang, L., Duff, M. O., Graveley, B. R., Carmichael, G. G. & Chen, L. L. Genomewide characterization of non-polyadenylated RNAs. *Genome Biol.* **12**, R16 (2011).
99. Marzluff, W. F., Wagner, E. J. & Duronio, R. J. Metabolism and regulation of canonical histone mRNAs: life without a poly(A) tail. *Nat. Rev. Genet.* **9**, 843–854 (2008).
100. Conrad, N. K., Mili, S., Marshall, E. L., Shu, M. D. & Steitz, J. A. Identification of a rapid mammalian deadenylation-dependent decay pathway and its inhibition by a viral RNA element. *Mol. Cell* **24**, 943–953 (2006).

101. Conrad, N. K., Shu, M. D., Uyhazi, K. E. & Steitz, J. A. Mutational analysis of a viral RNA element that counteracts rapid RNA decay by interaction with the polyadenylate tail. *Proc. Natl Acad. Sci. USA* **104**, 10412–10417 (2007).
102. Conrad, N. K. & Steitz, J. A. A. Kaposi's sarcoma virus RNA element that increases the nuclear abundance of intronless transcripts. *EMBO J.* **24**, 1831–1841 (2005).
103. Brown, J. A., Valenstein, M. L., Yario, T. A., Tycowski, K. T. & Steitz, J. A. Formation of triple-helical structures by the 3′-end sequences of MALAT1 and MENβ noncoding RNAs. *Proc. Natl Acad. Sci. USA* **109**, 19202–19207 (2012).
104. Wilusz, J. E. *et al.* A triple helix stabilizes the 3′ ends of long noncoding RNAs that lack poly(A) tails. *Genes Dev.* **26**, 2392–2407 (2012).
105. Sunwoo, H. *et al. MEN ε/β* nuclear-retained non-coding RNAs are up-regulated upon muscle differentiation and are essential components of paraspeckles. *Genome Res.* **19**, 347–359 (2009).
106. Wilusz, J. E., Freier, S. M. & Spector, D. L. 3′ end processing of a long nuclear-retained noncoding RNA yields a tRNA-like cytoplasmic RNA. *Cell* **135**, 919–932 (2008).
107. Tycowski, K. T., Shu, M. D. & Steitz, J. A. Myriad triple-helix-forming structures in the transposable element RNAs of plants and fungi. *Cell Rep.* **15**, 1266–1276 (2016).
108. Kierzek, E. & Kierzek, R. The thermodynamic stability of RNA duplexes and hairpins containing N^6-alkyladenosines and 2-methylthio-N^6-alkyladenosines. *Nucleic Acids Res.* **31**, 4472–4480 (2003).
109. Roost, C. *et al.* Structure and thermodynamics of N^6-methyladenosine in RNA: a spring-loaded base modification. *J. Am. Chem. Soc.* **137**, 2107–2115 (2015).
110. Heraud-Farlow, J. E. & Kiebler, M. A. The multifunctional Staufen proteins: conserved roles from neurogenesis to synaptic plasticity. *Trends Neurosci.* **37**, 470–479 (2014).
111. Csepany, T., Lin, A., Baldick, C. J. Jr & Beemon, K. Sequence specificity of mRNA N^6-adenosine methyltransferase. *J. Biol. Chem.* **265**, 20117–20122 (1990).
112. Horowitz, S., Horowitz, A., Nilsen, T. W., Munns, T. W. & Rottman, F. M. Mapping of N^6-methyladenosine residues in bovine prolactin mRNA. *Proc. Natl Acad. Sci. USA* **81**, 5667–5671 (1984).
113. Liu, N. *et al.* Probing N^6-methyladenosine RNA modification status at single nucleotide resolution in mRNA and long noncoding RNA. *RNA* **19**, 1848–1856 (2013).

Acknowledgements
A.K. is supported by grants from the US National Institutes of Health (R01HL126845), the March of Dimes (5-FY14-112) and the Center for Advanced Study at the University of Illinois, Chicago, USA. T.P. is supported by the US National Institutes of Health (R01GM113194). The authors apologize to those whose work could not be cited owing to space restraints.

Competing interests statement
The authors declare no competing interests.